Cellular Signalling 24 (2012) 2237–2248

Contents lists available at SciVerse ScienceDirect

Cellular Signalling

journal homepage: www.elsevier.com/locate/cellsig

Ras and Rap1 govern spatiotemporal dynamic of activated ERK in pituitary living cells

Caroline Zeiller [a], Marie-Pierre Blanchard [a], Morgane Pertuit [b], Sylvie Thirion [a], Alain Enjalbert [a,b], Anne Barlier [a,b], Corinne Gerard [a,*]

[a] Aix-Marseille Université, CNRS, CRN2M UMR 7286, 13344 cedex 15, Marseille, France
[b] AP HM, Conception, Laboratory of Molecular Biology, 13385, Marseille, France

ARTICLE INFO

Article history:
Received 3 May 2012
Received in revised form 2 August 2012
Accepted 14 August 2012
Available online 23 August 2012

Keywords:
ERK signalling
Ras
Rap1
Pituitary
EKAR
FRET

ABSTRACT

The Ras/Raf/MEK/ERK is a conserved signalling pathway involved in the control of fundamental cellular processes. Despite extensive research, how this pathway can process a myriad of diverse extracellular inputs into substrate specificity to determine biological outcomes is not fully understood. It has been established that the ERK1/2 pathway is an integrative point in the control of the pituitary function exerted by various extracellular signals. In addition we previously established that the GTPases Ras and Rap1 play a key role in the regulation of ERK1/2-dependent prolactin transcription by EGF or the cAMP-dependent neuropeptide VIP. In this report, using the FRET-based biosensor of ERK activity (EKAR) in the pituitary GH4C1 cell line, we show that both EGF and VIP tightly control the spatiotemporal dynamic of activated ERK with different magnitude and duration. Importantly, we provide the first evidence of a differential control of cytoplasmic and nuclear pools of activated ERK by the GTPases Ras and Rap1. Ras is required for nuclear magnitude and duration of EGF-dependent ERK activation, whereas it is required for both VIP-activated cytoplasmic and nuclear ERK pools. Rap1 is exclusively involved in VIP-activated ERK nuclear pool. Moreover, consistent with the control of the nuclear pool of activated ERK by the GTPases, we observe the same differential role of Ras and Rap1 on ERK nuclear translocation triggered by EGF or VIP. Together these findings identify Ras and Rap1 as determinant partners in shaping nuclear and cytoplasmic ERK kinetics in response to EGF and VIP, which in turn should control pituitary secretion.

1. Introduction

The Ras/Raf/MEK (MAPKinase and ERK Kinase)/ERK (extracellularly regulated kinase) is a highly evolutionary conserved signalling pathway [1] that is involved in the control of fundamental cellular processes that include cell proliferation, survival, apoptosis, differentiation, motility and metabolism [2–5]. Dysregulation of this signalling pathway is associated with a large range of pathological disorders [6]. In particular, ERK1/2 signalling abnormalities, many of which resulting from activating Ras or Raf mutations, occur in about 30% of human cancers [7]. For these reasons, the ERK pathway has been a focus of intensive research. The essential biochemistry of this pathway is now established, but how the pathway can process a myriad of specific extracellular inputs into diverse biological outputs is not yet fully understood. Recently, accumulating evidences have shown that duration, magnitude and subcellular compartmentalization of ERK activity could determine substrate specificity and biological outcomes [8–12].

In this regard, ERK is retained in the cytoplasm of resting cells, mainly due to interaction with its upstream activator MEK. Upon activation, ERK could or not translocate into the nucleus depending on its interaction with scaffold proteins such as PEA15, Sef, MEK partner 1 (MP1), paxillin or β arrestin which retain active ERK to different cytoplasmic compartments [13–15]. ERK nuclear translocation requires activation of MEK, ERK activation and acceleration of ERK shuttling between cytoplasm and nucleus [16,17]. Recently, Zehorai et al. have identified a nuclear translocation sequence on ERK, the SPS domain [18,19]. All together these mechanisms control the dynamic of the subcellular localization of ERK and contribute to the regulation of specific substrates upon stimulation. Besides determining the localization of the components of the ERK pathway, other scaffold proteins such as the kinase suppressor of Ras (KSR) and the connector enhancer of KSR (CNK) regulate the magnitude of ERK activation [20] whereas the dual specificity phosphatases (DUSPs) influence ERK temporal signalling [21].

Ras and Rap1 proteins are small GTPases that operate as molecular switches upstream of the Raf/MEK/ERK cascade. The differential

Abbreviations: MAPK, mitogen-activated protein kinase; MEK, mitogen-activated protein kinase/extracellular signal-regulated kinase kinase; ERK1/2, extracellularly regulated kinases 1 and 2; YFP, yellow fluorescent protein; CFP, cyan fluorescent protein; EKAR, extracellular signal-regulated kinase activity reporter; FRET, fluorescence resonance energy transfer; cAMP, cyclic adenosine monophosphate; VIP, vasoactive intestinal polypeptide; EGF, epidermal growth factor; NGF, nerve growth factor; PRL, prolactin.

* Corresponding author at: CRN2M, UMR 7286, Faculté de Médecine secteur Nord, CS80011, Bd Pierre Dramard, 13344 Marseille cedex 15, France. Tel.: +33 4 91 69 89 21; fax: +33 4 91 69 89 20.
E-mail address: corinne.gerard@univ-amu.fr (C. Gerard).

0898-6568/$ – see front matter © 2012 Elsevier Inc. All rights reserved.
http://dx.doi.org/10.1016/j.cellsig.2012.08.006

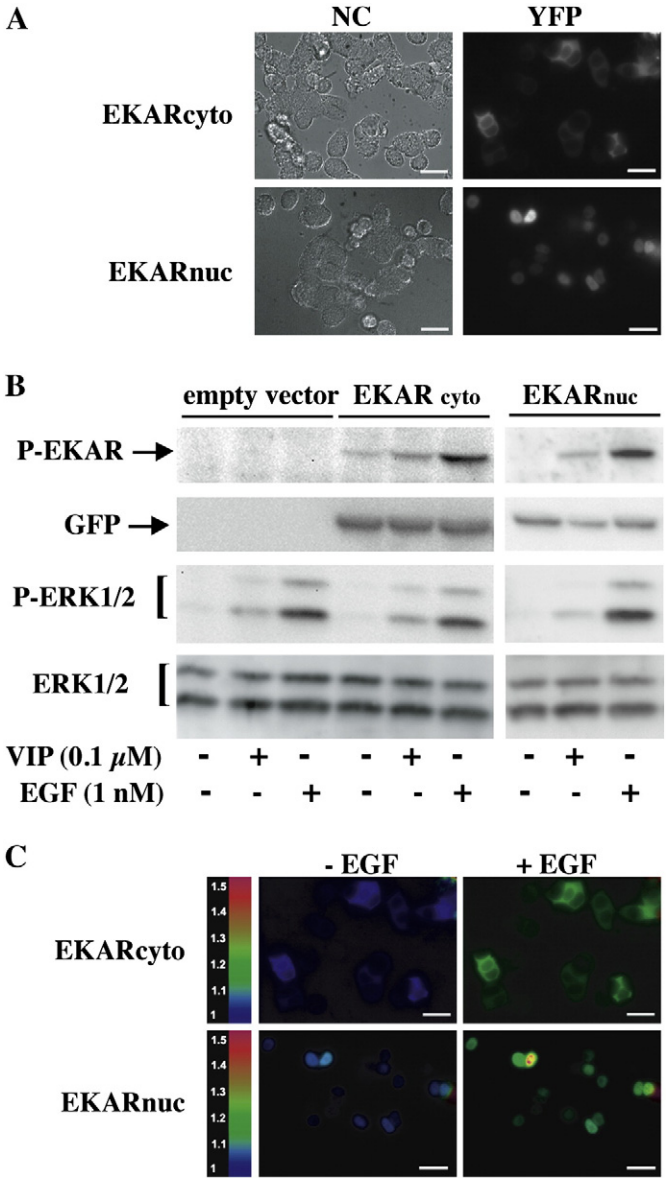

Fig. 1. Expression and function of EKAR sensors in pituitary GH4C1 cells. (A) GH4C1 cells were transfected for 48 h with 0.5 μg of $EKAR_{cyto}$ (upper panel) or $EKAR_{nuc}$ (lower panel). Right panels show cytoplasmic and nuclear YFP fluorescence respectively. Left panels show the corresponding Nomarski contrast (NC) fields. Scale bar: 20 μm. (B) Immunodetection of P-EKAR, total EKAR (GFP), P-ERK1/2 and total ERK1/2 as indicated (respectively from upper to lower panel), in cells transfected with $EKAR_{cyto}$ or $EKAR_{nuc}$ or the empty vector (pRK5) and treated 5 min in the absence or in the presence of 1 nM EGF or 0.1 μM VIP. (C) Pseudocolour images of the YFP/CFP emission ratios before (left panels) and after 1 nM EGF treatment for 5 min (right panels) in GH4C1 cells expressing $EKAR_{cyto}$ (upper panels) or $EKAR_{nuc}$ (lower panels). Scale bars 20 μm.

recruitment of these small GTPases is determinant in the control of cell proliferation by growth factors or hormonal stimulation of the cyclic adenosine monophosphate (cAMP) [22]. In the well studied rat pheochromocytoma cell line PC12, the epidermal growth factor (EGF) induces transient ERK activation and cell proliferation whereas the nerve growth factor (NGF) induces sustained ERK activation and triggers neuronal differentiation. Both EGF and NGF induce transient Ras activation but NGF also leads to sustained Rap1 activation [23,24]. Recently it has been shown that compartmentalized oncogenic mutants of H-Ras transform NIH3T3 cells with different efficiencies [25]. Thus the GTPases Ras and Rap1 might be important partners of spatiotemporal ERK dynamic.

Our and other's previous data on pituitary cell lines have provided evidence that the ERK1/2 cascade plays a central role in the control of pituitary function exerted by neuropeptides and growth factors [26–31]. In addition, we previously established that the specific activation of the GTPases Ras and Rap1 is crucial to the activation of the ERK1/2 cascade by growth factors or cAMP-dependent neuropeptides and that the differential recruitment of those monomeric G proteins plays a key role in the fine regulation of the prolactin (PRL) gene. EGF-dependent Ras activation increases PRL gene transcription whereas vasoactive intestinal polypeptide (VIP)-dependent Ras activation acts as a repressor of the PRL gene regulation. On the contrary, VIP-dependent Rap1 activation leads to an increase in PRL transcription [32].

In this context, we postulate that the GTPases Ras and Rap1 could play a crucial role in the spatiotemporal dynamic of the ERK pathway, in pituitary cells, under the control of growth factors or neuropeptides. Therefore, we conducted experiments to test this hypothesis directly, using single cell imaging in the differentiated GH4C1 pituitary living cells and the recently developed genetically encoded Fluorescence Resonance Energy Transfer (FRET)-based sensor of ERK activity (EKAR) [33]. Our results show that: (i) Both EGF and VIP specifically control the cytoplasmic and nuclear pools of activated ERK with magnitude and duration depending on the activated receptor. (ii) Ras activation is required for the EGF-dependent dynamic of nuclear ERK, whereas it is involved in both VIP-activated ERK cytoplasmic and nuclear pools. Rap1 activation is strictly required for nuclear ERK dynamic in response to VIP. Moreover, following YFP-ERK mobility in living cells, we provide evidence for a differential role of Ras and Rap1 on ERK nuclear translocation triggered by EGF or VIP.

2. Materials and methods

2.1. Reagents and plasmids

The vasoactive intestinal polypeptide (VIP) was purchased from Polypeptide Laboratories (Strasbourg, France). Epidermal growth factor (EGF) and UO126 were obtained from Promega (Charbonnière-les-Bains, France). Lipofectamine and cell culture reagents were from Invitrogen (Cergy-Pontoise, France). All other reagents were purchased from Sigma-Aldrich (St. Quentin Fallavier, France). The extracellular signal-regulated kinase activity reporters (EKAR sensors) were purchased from Addgene (Cambridge, MA, USA). The pCDNA3.1RasN17 expression vector was constructed by subcloning the BamHI/HindIII fragment of the pRSVH17 plasmid [34], containing the coding sequence of RasN17, into the polylinker of pCDNA3.1 expression vector (Invitrogen). The construct was verified by sequencing.

2.2. Cell culture and transfections

The somatolactotroph GH4C1 cell line (a generous gift of Dr Sobel, France) grown in Ham's F10 medium supplemented with 15% horse serum, 2.5% fetal calf serum (Eurobio, Les Ulis, France), penicillin (50 U/ml) and streptomycin (50 μg/ml), was kept at 37 °C in a water-saturated atmosphere containing 5% CO_2 and subcultured weekly. Transfections were performed 4–5 days after plating in six-well tissue culture plates or on poly-lysine coated glass coverslips respectively for immunoblot analysis or live imaging. For FRET experiments, cells were transfected for 48 h with 0.5 μg of the CFP-YFP version of the nuclear or cytoplasmic sensor EKAR using the lipofectamine reagent in line with the manufacturer's protocol (Invitrogen, France). In some experiments, cells were cotransfected with the EKAR sensors or 1 μg of pCDNA.I/

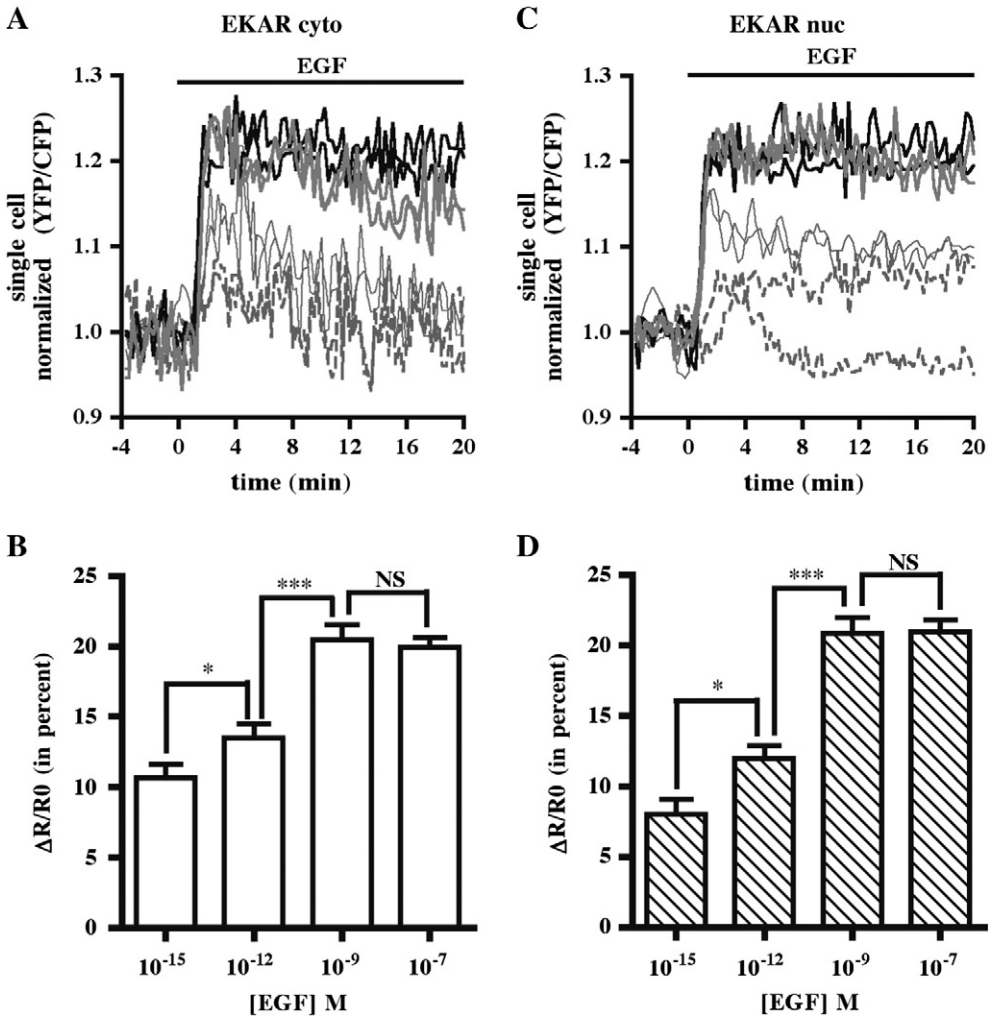

Fig. 2. Cytoplasmic and nuclear ERK activities are EGF dose-dependent in GH4C1 cells. GH4C1 cells expressing $EKAR_{cyto}$ (A, B) or $EKAR_{nuc}$ (C, D) were treated with increasing concentrations of EGF. (A, C) Traces represent the time courses of single cell recordings. Representative normalized YFP/CFP emission ratios were given for 2 cells at each concentration: 10^{-15} M (dotted thin grey line); 10^{-12} M (thin grey line); 10^{-9} M (black line); 10^{-7} M (dark grey line). (B, D) Bar graph depicts the magnitude (ΔR/R0) of $EKAR_{cyto}$ or $EKAR_{nuc}$ response to increasing concentrations of EGF as indicated, for at least 30 cells per dose. (*) $p<0.05$; (***) $p<0.001$.

HA-tagged ERK1 [35] to analyse ERK activation in whole cell extracts and 0.4 μg of pCDNA3.1RasN17 (dominant-negative mutant of Ras) or 2 μg of pRK5Rap1N17 (dominant-negative mutant of Rap1; [36]) or the respective empty vectors. To assess ERK nuclear translocation, cells were cotransfected with an equal amount (0.5 μg) of pEYFP-ERK [16] and pCMV-HA-MEK constructs to maintain transfected YFP-ERK in the cytoplasm of resting cells [16,37]. Cells were serum-starved in Ham's F10 medium for the last 15 h prior to each experiment. The transfection efficiencies were estimated at 45 ± 5% and 47 ± 4% for cytoplasmic EKAR and for nuclear EKAR respectively and at 46 ± 6% for YFP-ERK.

2.3. Live cell imaging

Experiments were carried out on an inverted microscope (Axiovert 200, Zeiss, Germany) using a 63× oil-immersion objective. 12 bit grey level images were collected with a cooled CCD camera (CoolSnapHQ, Roper Scientific, France) under MetaMorph software control (Universal Imaging Corporation). For imaging, culture medium was replaced by modified Earle's salt solution containing 137 mM NaCl, 5.4 mM KCl, 0.4 mM Na_2HPO_4, 0.8 mM $MgSO_4$, 5.5 mM glucose, 1.8 mM $CaCl_2$, and 20 mM Hepes (pH 7.4), at least 30 min before recording. Agonists and/or inhibitor (VIP, EGF, 5 μM U0126) were locally perfused to the analyzed areas. Band-pass filter sets (Chroma) for FRET detection were 436/20 for excitation and 480/40 and 535/30 for CFP and YFP emission respectively. The filter set for YFP-ERK fluorescence recording was 500/20 for excitation and 535/30 for emission. In the established recording conditions, the absolute intensity of the fluorophores remained stable throughout the whole experiment.

2.4. Immunoblot analysis

Transfected GH4C1 cells grown for 2 days in six-well tissue culture plates were preincubated for 30 min in Ham's F10 medium supplemented with 20 mM HEPES (pH 7.4). Cells were then treated for 5 min with or without 0.1 μM VIP or 1 nM EGF and/or 5 μM U0126 and solubilized at 4 °C for 20 min in the lysis buffer previously described by Harvey et al. [33] containing [25 mM Hepes (pH 7.4), 134 mM NaCl, 1% Triton X100, 10% glycerol, 25 mM βglycerophosphate, 2 mM EDTA, 1 mM 4-(2-aminoethyl) benzenesulfonyl fluoride (AEBSF), 1 mM Na_3VO_4, and 10 μg/ml

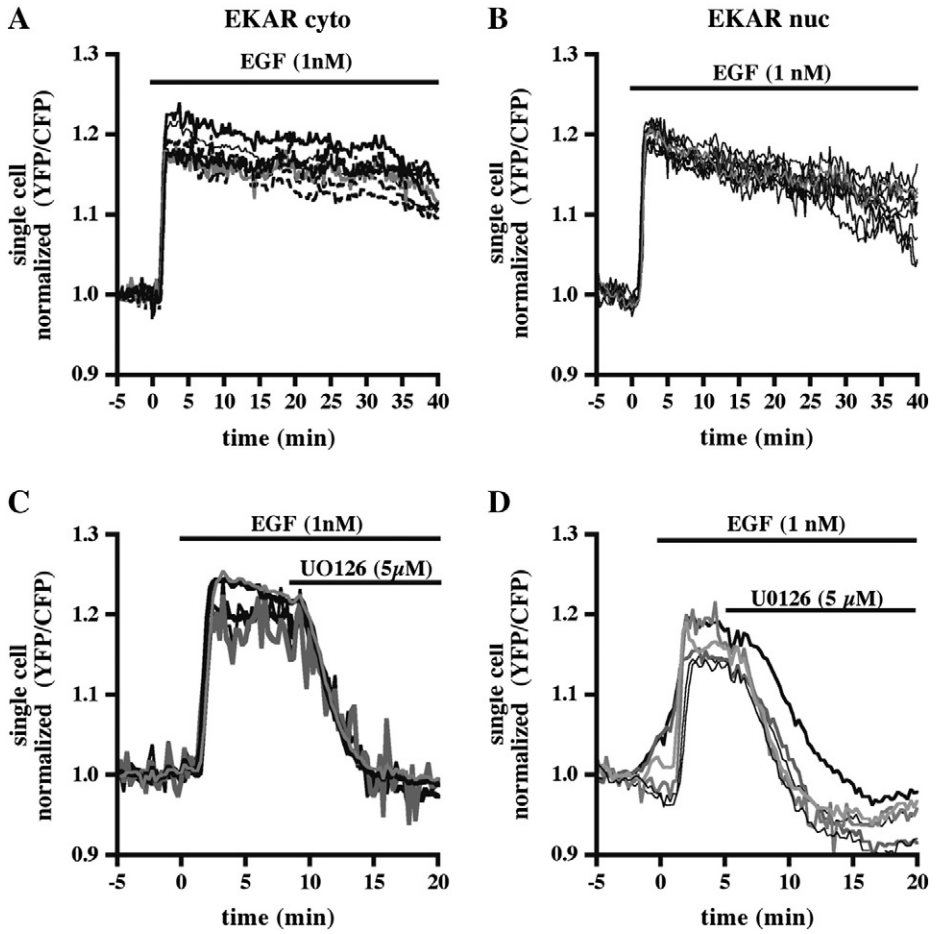

Fig. 3. EGF regulates spatiotemporal ERK activity in GH4C1 cells. GH4C1 cells expressing $EKAR_{cyto}$ (A, C) or $EKAR_{nuc}$ (B, D) were treated with 1 nM EGF alone (A, B) or with 1 nM EGF followed by 5 μM U0126 as indicated (C, D). Traces represent the time courses of single cell recordings. Normalized YFP/CFP emission ratios were given for n cells, with n = 7, 10, 5, and 6 respectively in A, B, C, and D.

leupeptin and aprotinin]. Denatured proteins were separated on SDS-PAGE and transferred to PVDF membrane (Perkin Elmer, France). Immunodetections of P-EKAR and P-ERK1/2 were respectively performed using a polyclonal Phospho-cdc25 (Thr48) and polyclonal P-ERK1/2 antibodies (New England Biolab, Ozyme, France) and an anti-Rabbit IgG coupled to alkaline phosphatase as the secondary antibody. Blots were developed with the enhanced chemiluminescence CDP-Star™ detection system (Applied Biosystems, France) and quantified with a GeneGnome (Ozyme, France). Total EKAR and ERK1/2 contents were systematically monitored by reprobing the membrane using a mouse monoclonal GFP antiserum (Roche Diagnostic, Meylan, France) and a rabbit polyclonal ERK1 antiserum (Santa Cruz Biotechnology, Tebu, France). The levels of transfected mutants of Ras and Rap1 were monitored using anti-Ras or anti-Rap1 mouse monoclonal antibodies (BD Transduction Laboratories, Interchim, France). Expression of RasN17 and Rap1N17 were 2.7 ± 0.6 ($n = 6$) and 2.0 ± 0.5 ($n = 5$) fold those of the endogenous Ras and Rap1 proteins respectively.

2.5. Data analysis

For each FRET experiment, imaging was realized on at least three distant areas of the cell culture mentioned as region of interest (ROI) from three different dishes. Each ROI contained 7–10 EKAR expressing cells. Single cell ratiometric fluorescence measurements were used to analyze FRET signals reported by EKAR. The kinetics of YFP and CFP emissions were measured in the whole nucleus or in the whole cytoplasm of each individual cell. Measured grey values were then exported to Microsoft Excel software for further processing: background intensity was subtracted prior to YFP/CFP emission intensity ratios calculation. These ratios were finally normalized to the initial ratio value (R0) determined as the mean of the YFP/CFP emission intensity ratios of the first 20 images before drug perfusion. To better characterize the kinetic of the YFP/CFP emission ratio, the magnitude of the response (ΔR/R0) was calculated as $\Delta R/R0 = (Rmax - R0)/R0 \times 100$, where Rmax is the maximal YFP/CFP ratio after agonist application. The time of maximal activation (Tmax), which corresponds to the time to achieve Rmax, was determined. We also calculated the half time of inactivation (T1/2), which corresponds to the time to return to Rmax/2. Results were expressed as the time course of single cell normalized YFP/CFP (Figs. 2, 3, 5 and 6) or as mean ± SEM of normalized YFP/CFP of different cells (Figs. 7 and 10). Statistical analysis was determined using one-way ANOVA and differences were considered to be significant at $P \leq 0.05$.

The time course of ERK nuclear translocation was analyzed in at least 16 cells from at least two independent dishes by recording YFP fluorescence intensity changes in the nucleus upon stimulation by VIP or EGF. Results were expressed as variations of fluorescence intensities reported to the initial value (F/F0).

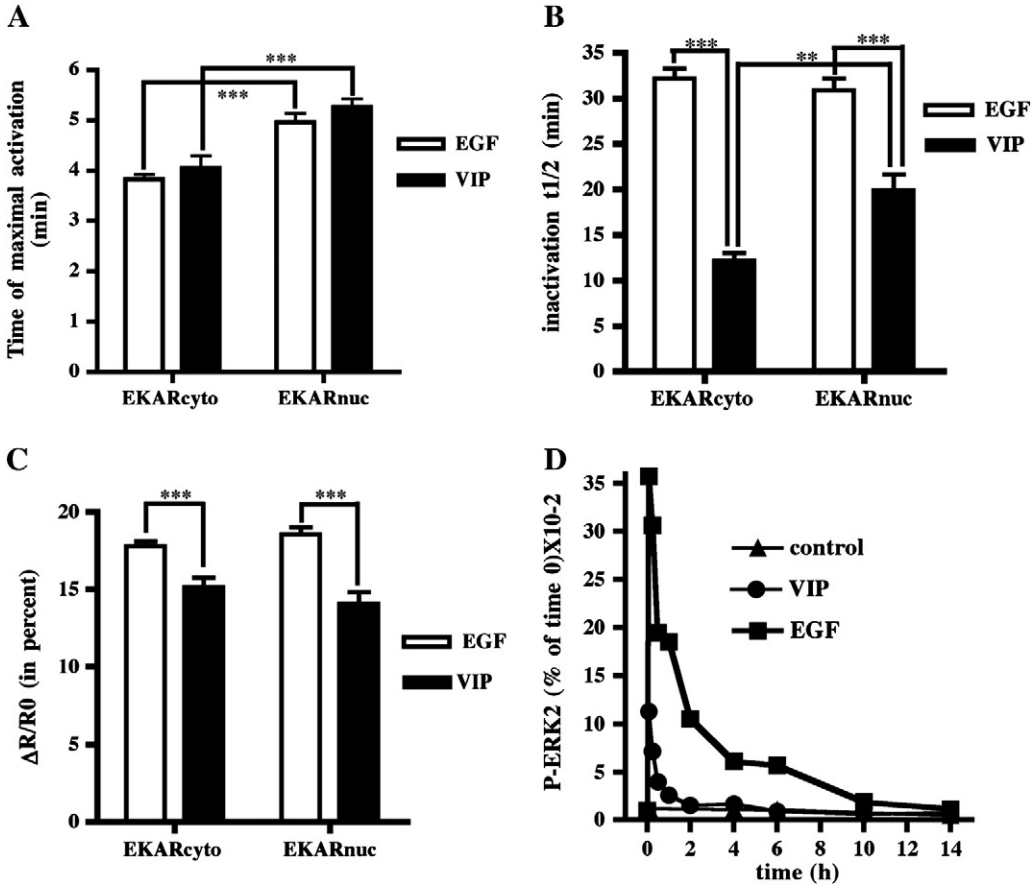

Fig. 4. Quantification of the kinetic parameters of $EKAR_{cyto}$ and $EKAR_{nuc}$ responses to EGF and VIP. (A, B, C) Single cell recordings of GH4C1 cells expressing $EKAR_{cyto}$ or $EKAR_{nuc}$ were performed as described in Fig. 3 on at least 30 cells for each condition. Cells were treated with 1 nM EGF or 0.1 μM VIP. The kinetic parameters were calculated as described in the Materials and methods and were given as mean ± SEM. (A) Bar graph depicts the time of maximal $EKAR_{cyto}$ or $EKAR_{nuc}$ response to EGF or VIP. (B) Bar graph depicts the half time of $EKAR_{cyto}$ or $EKAR_{nuc}$ inactivation in response to EGF or VIP. (C) Bar graph depicts the magnitude (ΔR/R0) of $EKAR_{cyto}$ or $EKAR_{nuc}$ response to EGF or VIP. (**) $p<0.01$; (***) $p<0.001$. (D) Time course of GH4C1 endogenous P-ERK2 activation in the presence of 1 nM EGF or 0.1 μM VIP determined as described in the Materials and methods on whole cell lysates.

3. Results

3.1. Expression and function of the FRET-based sensor EKAR, in pituitary living cells

With a view to determine the spatiotemporal dynamic of ERK, under the control of growth factors and neuropeptides, in the GH4C1 cell line, we have used the genetically encoded fluorescent sensor of ERK activity EKAR previously described by Harvey et al. [33]. The somatolactotroph GH4C1 cell line transfected either with the cytoplasmic form of the sensor ($EKAR_{cyto}$) or the nuclear one ($EKAR_{nuc}$) showed restricted localization respectively to the cytoplasm or to the nucleus (Fig. 1A). To test the sensor's function, GH4C1 cells expressing one of the two forms of the sensor were first stimulated 5 min with 1 nM EGF or 0.1 μM VIP, which have been previously shown to activate ERK1/2 in pituitary cells [29,32,38]. In these conditions, biochemical analysis of whole cell lysates showed that the phosphorylation of both $EKAR_{cyto}$ and $EKAR_{nuc}$ was increased in the presence of EGF or VIP and was associated to an increase in Phospho-ERK1/2 (Fig. 1B). Moreover, in the same conditions, agonist treatments induced an increase in FRET signals in both cytoplasmic and nuclear compartments of GH4C1 living cells, as illustrated in the presence of 1 nM EGF (Fig. 1C). These results demonstrate that the previously developed EKAR sensors [33] are powerful tools for the analysis of spatiotemporal ERK signalling in the pituitary living cells GH4C1 and show a good relationship between ERK1/2 phosphorylation, EKAR phosphorylation and FRET signals.

3.2. EGF regulates spatiotemporal ERK signalling

It has been previously shown that EGF-dependent ERK1/2 activation is involved in the control of diverse pituitary functions as PRL secretion or cell survival [32,39]. So to elucidate the critical role of ERK activity in establishing the specificity of downstream outputs, we have explored the spatiotemporal dynamic of ERK, by recording FRET signal changes in the presence of EGF, in GH4C1 living cells using both $EKAR_{cyto}$ and $EKAR_{nuc}$ sensors. Single cell recordings of FRET signals progressively enhanced in both $EKAR_{cyto}$ or $EKAR_{nuc}$ expressing cells treated with increasing concentrations of EGF (Fig. 2A, C). Maximal amplitude of EKAR FRET signals (ΔR/R0) is observed in the presence of 1 nM EGF in both compartments (Fig. 2B, D). When cells were stimulated with 1 nM EGF, all cells transfected with the same sensor showed a similar rapid and substantial increase in the YFP/CFP emission ratio, which reached a plateau in several minutes (Fig. 3A, B). The emission ratio returned to the baseline levels in both compartments after 5 μM U0126 treatment (a specific inhibitor of the ERK pathway) (Fig. 3C, D). Moreover, pretreatment of cells with 5 μM U0126 completely abolished EGF-induced FRET response of EKAR (not shown). We have verified that simultaneous treatment with EGF and U0126 suppressed the phosphorylation of $EKAR_{cyto}$ and $EKAR_{nuc}$ in whole cell extracts (not shown). So FRET signal changes, observed in the presence of EGF, correlated to the activation of the endogenous ERK in both compartments. The Tmax of EKAR FRET signal was observed within less than 4 min in the cytoplasm

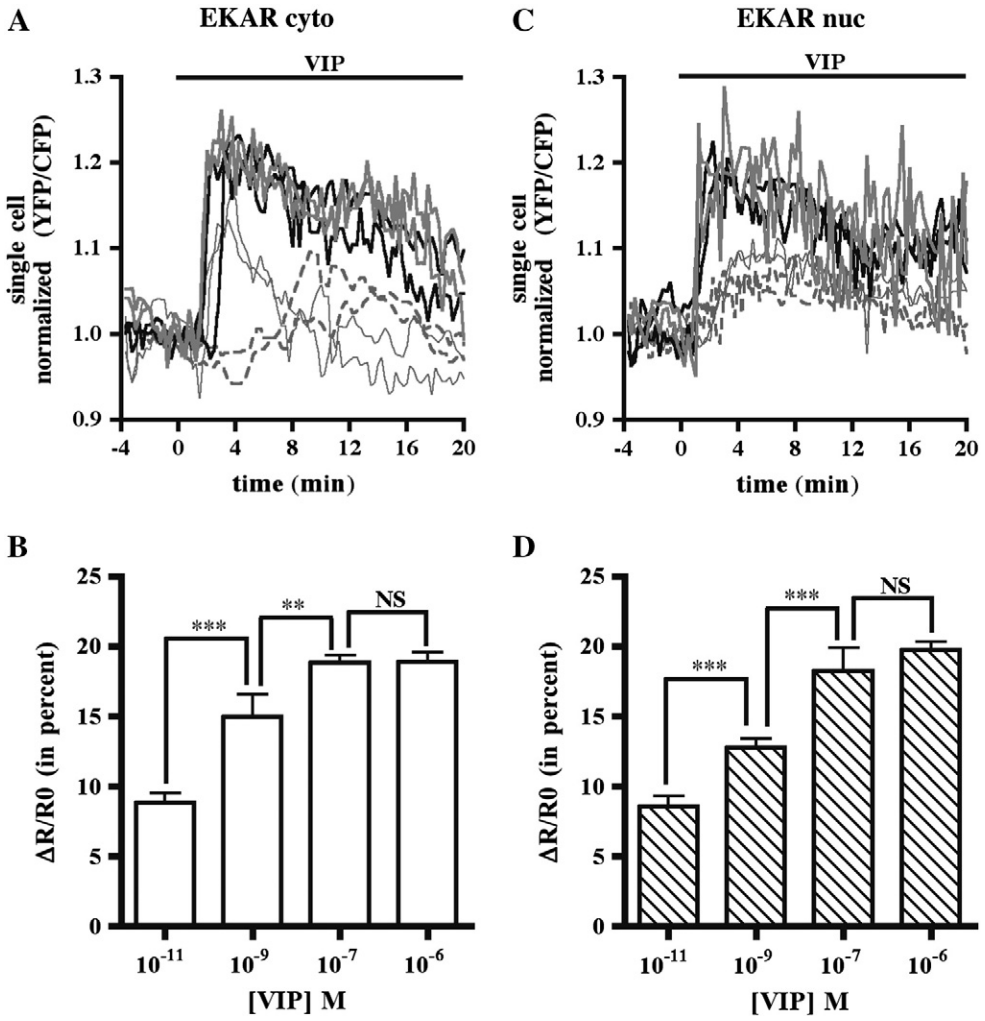

Fig. 5. Cytoplasmic and nuclear ERK activities are VIP dose-dependent in GH4C1 cells. GH4C1 cells expressing $EKAR_{cyto}$ (A, B) or $EKAR_{nuc}$ (C, D) were treated with increasing concentrations of VIP. (A, C) Traces represent the time courses of single cell recordings. Representative normalized YFP/CFP emission ratios were given for 2 cells at each concentration: 10^{-11} M (dotted thin grey line); 10^{-9} M (thin grey line); 10^{-7} M (black line); 10^{-6} M (dark grey line). (B, D) Bar graph depicts the magnitude (ΔR/R0) of $EKAR_{cyto}$ or $EKAR_{nuc}$ response to increasing concentrations of VIP as indicated, for at least 30 cells per dose. (**) $p<0.01$; (***) $p<0.001$.

and was significantly enhanced in the nucleus (Fig. 4A). EKAR FRET signal then decreased slowly with a half time inactivation of more than 30 min in both compartments (Fig. 4B). There was no significant difference in the amplitude of the EKAR FRET signals (ΔR/R0) in both compartments (Fig. 4C). Taken together these results show that EGF activates ERK in both compartments with similar dose dependence, same time course and magnitude except an increase in the nuclear Tmax.

3.3. The cAMP pathway regulates spatiotemporal ERK signalling

It has been previously established that the regulation of the PRL gene by cAMP required crosstalk with the ERK1/2 cascade [29,30,32]. We have then examined the role of the cAMP pathway on the spatiotemporal dynamic of ERK. As described above, both $EKAR_{cyto}$ and $EKAR_{nuc}$ were phosphorylated in the presence of 0.1 μM VIP (known to stimulate the cAMP pathway via the VPAC2 receptor in the GH4C1 cell line [40]) and were associated to ERK1/2 activation. Single cell recordings of $EKAR_{cyto}$ or $EKAR_{nuc}$ FRET signals increased in a dose dependent manner in the presence of VIP (Fig. 5A, C). Maximal amplitude of EKAR FRET signals (ΔR/R0) is observed for 0.1 μM VIP in both compartments (Fig. 5B, D). In the presence of 0.1 μM VIP, EKAR FRET signal displayed a similar increase in the YFP/CFP emission ratio in each compartment (Fig. 6A, B). Post treatment with 5 μM U0126 induced a dramatic fall in the emission ratio as shown in the nucleus (Fig. 6C). As for EGF treatment, the Tmax of EKAR FRET signal was observed within 4 min in the cytoplasm and was increased in the nucleus (Fig. 4A). Time course of inactivation was significantly faster in the cytoplasm than in the nucleus of VIP-treated cells (Fig. 4B), whereas the amplitude of the FRET signals (ΔR/R0) was similar in both compartments (Fig. 4C).

The comparison of activated ERK dynamic triggered by 1 nM EGF or 0.1 μM VIP displays similar onset of ERK activation after both treatments in each compartment. However, ERK activation is more sustained in EGF treated GH4C1 cells than in VIP treated cells in both compartments due to increase in the inactivation half time in response to EGF. Moreover the ΔR/R0 were smaller in VIP treated cells (Fig. 4A, B, C). The spatiotemporal dynamic of activated ERK observed in single cell recordings of EKAR FRET signal was consistent with the time course of endogenous ERK activation in the presence of 1 nM EGF or 0.1 μM VIP measured in whole cell lysates (Fig. 4D).

3.4. Ras controls EGF-dependent activation of ERK nuclear pool

We previously established that activation of the GTPases Ras and Rap1 is crucial to the activation of the ERK1/2 cascade by EGF and the cAMP pathway, and that the differential recruitment of those

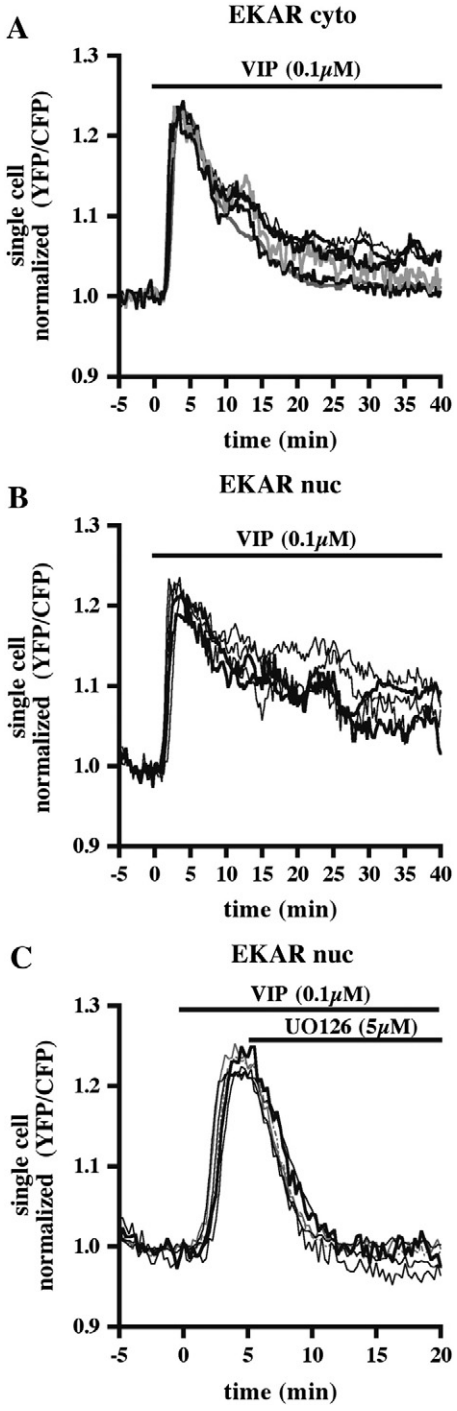

Fig. 6. VIP regulates spatiotemporal ERK activity in GH4C1 cells. GH4C1 cells expressing $EKAR_{cyto}$ (A) or $EKAR_{nuc}$ (B, C) were treated with 0.1 μM VIP alone (A, B) or with 0.1 μM VIP followed by 5 μM U0126 as indicated (C). Traces represent the time courses of single cell recordings. Normalized YFP/CFP emission ratios were given for n cells, with n = 6, 5, and 6 respectively in A, B, and C.

monomeric G proteins plays a key role in the regulation of pituitary function [32]. We therefore analyzed the role of Ras and Rap1 in the EGF-dependent spatiotemporal dynamic of ERK, by using the well characterized dominant negative forms of Ras and Rap1, respectively RasN17 and Rap1N17 [36,41]. Cotransfection of the dominant negative mutant of Rap1 (Rap1N17) either with $EKAR_{cyto}$ or $EKAR_{nuc}$ in GH4C1 cells, did not modify the time course of EGF-dependent FRET signal neither in the cytoplasm nor in the nucleus (Fig. 7A, B).

Expression of RasN17 cotransfected with $EKAR_{cyto}$ (Fig. 7C), only increased the Tmax of EGF-dependent ERK activation from 3.57 ± 0.25 min to 5.02 ± 0.25 min ($p<0.001$). Expression of RasN17, cotransfected with $EKAR_{nuc}$, altered the time course of FRET signal in the nucleus in response to EGF (Fig. 7D). RasN17 significantly increased the time observed to achieve maximal activation of ERK in the nucleus after EGF treatment and reduced both the half time of ERK inactivation and the amplitude of ERK activation (Fig. 8). In these experimental conditions, we have verified that alteration of the EGF-dependent FRET signal in the presence of RasN17, in the nucleus, was correlated to a decrease in $EKAR_{nuc}$ phosphorylation (Fig. 9A). On the contrary, the phosphorylation of $EKAR_{nuc}$ by EGF was not modified in the presence of Rap1N17 (Fig. 9B). In parallel experiments, we have explored the effects of RasN17 and Rap1N17 on EGF-dependent HA-ERK1 phosphorylation after cotransfection with the mutants, as previously described [32]. Fig. 9C shows that HA-ERK1 activation in the presence of EGF was largely depressed in RasN17 expressing cells whereas it was slightly affected by Rap1N17.

3.5. Ras and Rap1 both control VIP-dependent spatiotemporal ERK dynamic

In cells expressing Rap1N17, the time course of FRET signal was exclusively altered in the nucleus after VIP treatment (Fig. 10A, B). The time of maximal activation as well as the half time of inactivation of the nuclear pool of ERK were increased, whereas the amplitude of FRET signal was largely depressed (Fig. 11A). Whereas Ras controls the EGF-dependent nuclear pool of ERK, the time course of VIP-dependent ERK activation was altered in both compartments in RasN17 expressing cells (Fig. 10C, D). The time of maximal ERK activation was increased in both compartments (Fig. 11B, C). The half time of ERK inactivation was not significantly affected in the nucleus of RasN17 expressing cells (Fig. 11C), but was increased in the cytoplasm (Fig. 11B). Moreover, the amplitude of FRET signal was greatly depressed in both compartments (around 50%) in the presence of RasN17 (Fig. 11B, C). These results suggest that Ras controls nuclear and cytoplasmic duration and magnitude of the VIP-dependent ERK activity and that both GTPases Ras and Rap1 control VIP-dependent activation of the nuclear pool of ERK. In the same experimental conditions, RasN17 and Rap1N17 depressed VIP-dependent EKAR phosphorylation (Fig. 9A, B). Finally, in parallel experiments, performed on whole cell lysates of VIP treated cells, the activation of HA-ERK1 was similarly depressed in the presence of RasN17 or Rap1N17 (Fig. 9C).

3.6. Differential control of VIP-dependent and EGF-dependent ERK nuclear translocation by Ras and Rap1

It is now currently admitted that nuclear activation of ERK substrates requires activated ERK translocation into the nucleus. Because Ras and Rap1 controlled the nuclear pool of activated ERK we further analyzed the contribution of Ras and Rap1 to ERK nuclear translocation. According to previous data [17,37], YFP-ERK is mostly localized in the cytoplasm of resting cells (Fig. 12, Ctrl left column). Upon both EGF and VIP treatments, cells displayed a progressive increase in nuclear YFP-ERK which achieved a maximum in several minutes (Fig. 12, lanes A, D). Expression of RasN17 reduced and delayed the EGF-dependent nuclear translocation of YFP-ERK (Fig. 12, lane B) whereas it was not altered in the presence of Rap1N17 (Fig. 12, lane C). On the contrary, in VIP treated cells, the expression of both mutants largely depressed nuclear YFP-ERK (Fig. 12, lanes E, F).

4. Discussion

The idea that specific biological outcomes are determined by spatiotemporal distribution of activated key signalling partners has

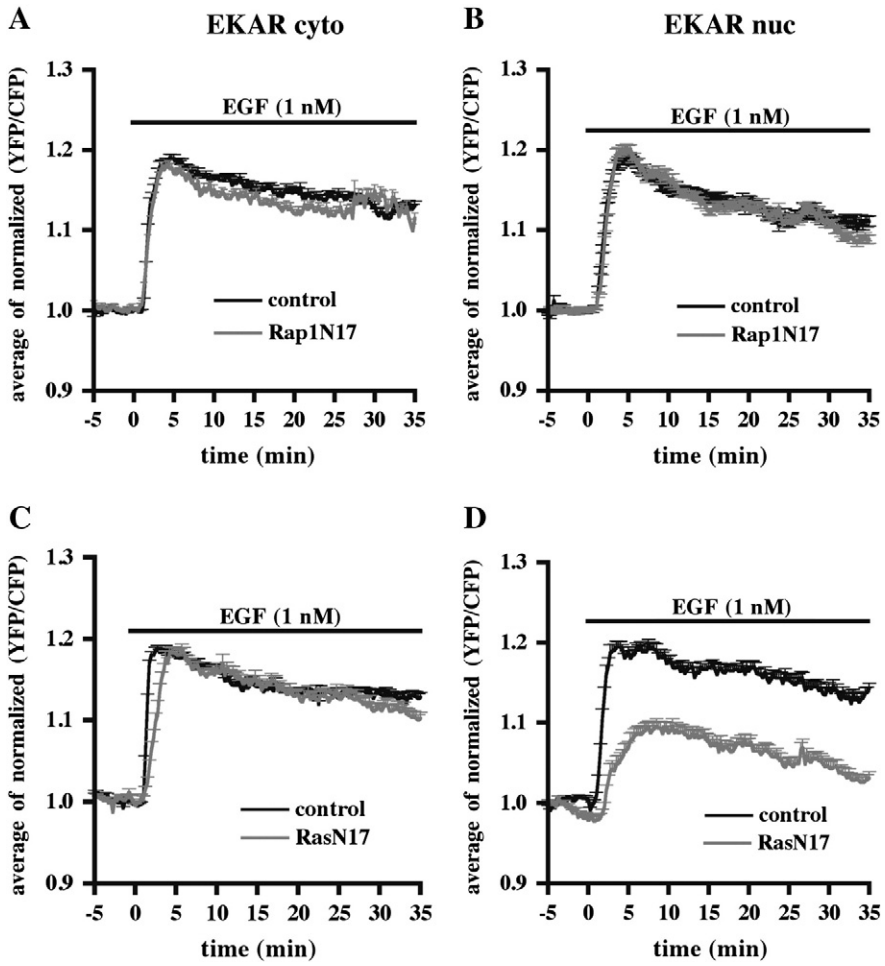

Fig. 7. Ras controls ERK nuclear pool activated by EGF. GH4C1 cells were cotransfected with $EKAR_{cyto}$ (A, C) and pRK5Rap1N17 (A) or pCDNA3.1RasN17 (C) or the respective empty vectors (control in A, C) or with $EKAR_{nuc}$ (B, D) and pRK5Rap1N17 (B) or pCDNA3.1RasN17 (D) or the respective empty vectors (control in B, D). Cells were treated with 1 nM EGF as indicated. Single cell recordings were performed on at least 30 cells for each condition. Traces represent the mean ± SEM of single cell recordings.

emerged from few years [11,42–44]. However, analysis of spatial behaviours of the ubiquitous MAPKinase ERK in living cells is starting to be explored with the recent development of genetically encoded FRET-based sensors. These ERK sensors have been validated in highly transformed proliferative cell lines (HEK293, MCF7, COS7…) stimulated by EGF [33,45,46]. They have been sparsely used to analyze the spatiotemporal dynamic of ERK signalling, in living cells, under biologically relevant conditions [33,47].

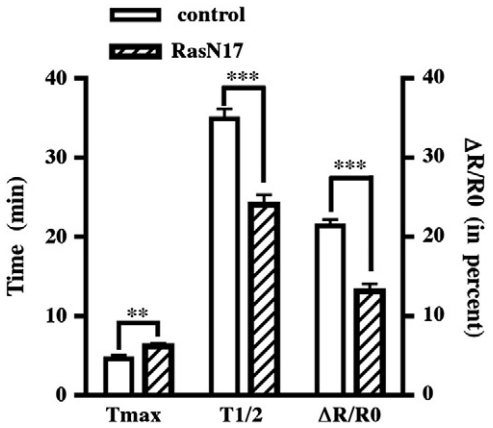

Fig. 8. Quantification of the kinetic parameters of $EKAR_{nuc}$ responses to EGF in RasN17 expressing GH4C1 cells. Single cell recordings of GH4C1 cells coexpressing $EKAR_{nuc}$ and pCDNA3.1RasN17 or the empty vector pCDNA3.1 (control) were performed and cells were treated with 1 nM EGF as described in Fig. 7 on at least 30 cells for each condition. The kinetic parameters Tmax, T1/2 and ΔR/R0 were calculated as described in the Materials and methods and were given as mean ± SEM. (**) $p<0.01$; (***) $p<0.001$.

Here, we have explored the spatiotemporal dynamic of ERK in the differentiated pituitary cell line GH4C1 which still retains regulated hormonal secretion and low growing rate [48]. We established for the first time that two physiological modulators of pituitary function (EGF and VIP) finely regulate the dynamic of cytoplasmic and nuclear pools of activated ERK in living cells. The GTPases Ras and Rap1, that encode the properties of activated VIP and EGF receptors, play a key role in shaping ERK response kinetics in both compartments.

Different methods have been devised for intracellular analysis of ERK signalling. Immunofluorescence microscopy using anti phospho-ERK antibodies has a poor temporal resolution. The fluorescent tagged-ERK protein is a useful tool to study ERK localization in living cells and to address ERK nuclear translocation. However, spatiotemporal information on activated ERK in living cells could be accessed only with FRET sensors. In agreement with the observations of Harvey et al. in HEK293 cells [33], we show that EKAR FRET signals induced by EGF or VIP treatment are reversible and rapidly depressed by UO126 treatment. These responses are closely associated to EKAR phosphorylation and endogenous ERK1/2 activation. EKAR FRET signal cannot be related to activation of other MAPKinase pathways as cAMP and EGF are not able to activate P38 and JNK kinases in GH4C1 cells ([49], C. Gerard, unpublished). Therefore, in pituitary cells, $EKAR_{cyto}$ and $EKAR_{nuc}$ selectively report the endogenous activity of ERK

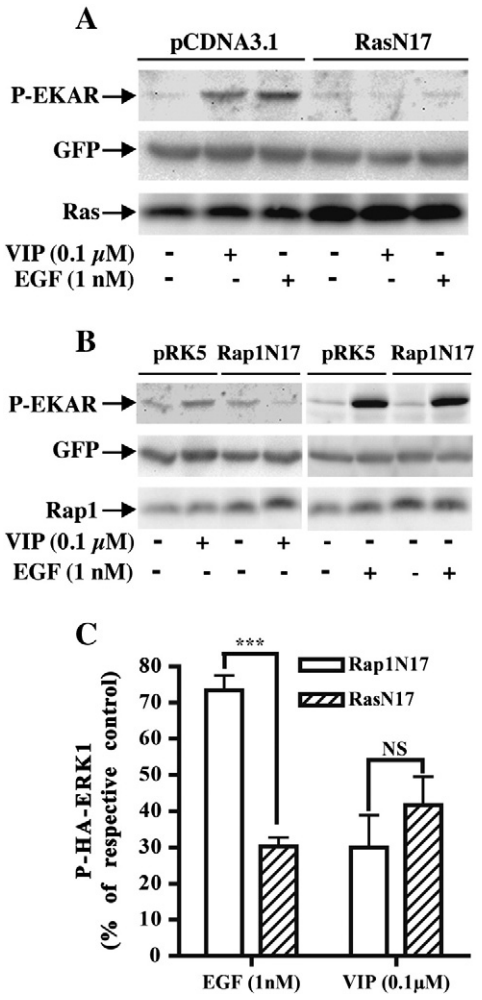

Fig. 9. Inhibition of EKAR FRET signals by Ras and Rap1 dominant negative mutants is associated to P-EKAR and P-HA-ERK decrease. GH4C1 cells were cotransfected with $EKAR_{nuc}$ and pCDNA3.1RasN17 or pCDNA3.1 (A) or with $EKAR_{nuc}$ and pRK5Rap1N17 or pRK5 (B) or cotransfected with HA-ERK1 and pRK5Rap1N17 or pRK5 or pCDNA3.1RasN17 or pCDNA3.1 (C). 48 hours after transfection, cells were treated with 1 nM EGF or 0.1 μM VIP during 5 min. Expression of phosphorylated EKAR (P-EKAR), total EKAR (GFP), Ras and Rap1 was performed on whole cell extracts as described in the Materials and methods. Representative immunoblots were given (A, B). Immunodetection of P-HA-ERK1 and HA-ERK1 was performed on cell lysates. Expression of P-HA-ERK1 normalized to the level of HA-ERK1 was performed as previously described [32] and was given as mean ± SEM of three determinations. (***) $p<0.001$ (C).

and its capacity to phosphorylate substrates in each compartment under physiological conditions.

Using these ERK sensors, it is shown that EGF and VIP specifically regulate spatiotemporal ERK dynamic. EGF and VIP dose-dependently activate cytoplasmic and nuclear pools of ERK, with similar profiles in both compartments for each agonist. These dose responses are consistent with the previously observed dose responses of endogenous ERK to EGF or VIP in whole cell lysates (C. Gerard, unpublished, [29]). The time courses of EGF-dependent ERK activation are similar in nuclear and cytoplasmic compartments but are clearly more sustained than the observed time courses of VIP-dependent ERK activation in the respective compartments. The reduced half times of ERK inactivation after VIP treatment could be in favour of an increase in the recruitment of phosphatases after activation of a cAMP pathway. In addition, under VIP activation, the duration of cytoplasmic ERK activity is shorter than in the nucleus. Activation of the protein kinase A (PKA) downstream of activated VPAC2 receptor [29,40,49] could regulate tyrosine phosphatase activities in the cytoplasm and favour activated-ERK nuclear translocation as previously reported in other cell types [50]. Both in the presence of EGF or VIP, an increased Tmax of about 1 min is observed in the nucleus in comparison to the cytoplasm. This could be related to nuclear translocation of activated ERK as we show that nuclear accumulation of YFP-ERK under stimulation take place with a delay of 1–2 min, which is consistent with previous observations in other cell types [17].

In the aim of understanding the mechanisms underlying the control of spatiotemporal activated ERK by EGF and VIP, we have examined the role of the GTPases Ras and Rap1 based on our previous experimental grounds [32,49]. We provide the first evidence of a differential control of cytoplasmic and nuclear pools of activated ERK by the GTPases Ras and Rap1. Ras is largely involved in the control of nuclear magnitude and duration of EGF-dependent ERK activation, whereas it slightly controls the onset of ERK activation in the cytoplasm. Moreover, expression of RasN17 reduces YFP-ERK accumulation in the nucleus triggered by EGF. Overall, these results highly suggest that Ras controls the fraction of activated ERK available for movement to the nucleus in the presence of EGF. In the same way, Rap1 seems to exclusively control the fraction of activated ERK available for nuclear import after VIP treatment. So the time to achieve maximal ERK activation as well as the amplitude of ERK activation in the nucleus may be at least partly controlled by Ras or Rap1-dependent ERK nuclear translocation, respectively after EGF or VIP treatment. Whereas Rap1 is strictly involved in the control of VIP-dependent ERK nuclear pool, Ras is involved in the control of both cytoplasmic and nuclear pools of activated ERK in response to VIP. In these conditions, it is not excluded that the effect of Ras on the cytoplasmic pool of activated ERK would modify the size of the activated ERK fraction available for nuclear import. So using EKAR FRET sensors (to selectively monitor ERK activity in the cytoplasm or in the nucleus) and YFP-ERK mobility in living cells (to analyse ERK nuclear translocation), we could conclude that Ras and Rap1 specifically contribute to the nucleocytoplasmic trafficking of ERK and to ERK activation in each compartment in response to EGF or VIP. It is widely recognized that the different isoforms of Ras as well as Rap1 have different regulated subcellular localizations and contribute to the establishment of active signalling platforms [51–54]. Moreover, it has been shown that the GTPase Ras could interact with specific scaffold proteins as MEKK1 and SUR-8 [55,56]. In this respect, Casar et al. have recently demonstrated that spatial regulation of ERK1/2 substrate specificity is dictated by the microlocalization of Ras and by the selection of specific scaffold proteins [57]. Further experiments are now required to determine the nature of the scaffold proteins which could account for Ras and Rap1 specificity regarding spatiotemporal ERK dynamic in GH4C1 cells.

The physiological relevance and the mechanisms underlying transient and sustained ERK activation, in response to growth factors, have been elucidated extensively in PC12 cells. It seems that the proteins involved in the sustained ERK activation and the neuronal differentiation triggered by NGF are distributed over the whole signal transduction network. Thus, endocytosis of the NGF receptor, sustained activation of Rap1 as well as involvement of the scaffold proteins Sef and KSR, which retain activated ERK in the cytoplasm, contribute to NGF-dependent sustained ERK activation [58–60]. Moreover, it has been recently shown that spatiotemporally regulated PKA activity contributes to the specific control of the duration of nuclear ERK activity induced by EGF and NGF [47]. In pituitary cells, activation of the cAMP pathway could induce a proliferative signal [61] whereas EGF triggers cell death [39]. In addition, cAMP-dependent neuropeptides and EGF both control hormonal secretion [38,39,62]. We have previously demonstrated that Ras and Rap1 are crucial components of ERK-dependent regulation of PRL secretion [28,32]. Therefore it is tempting to speculate that the spatiotemporal

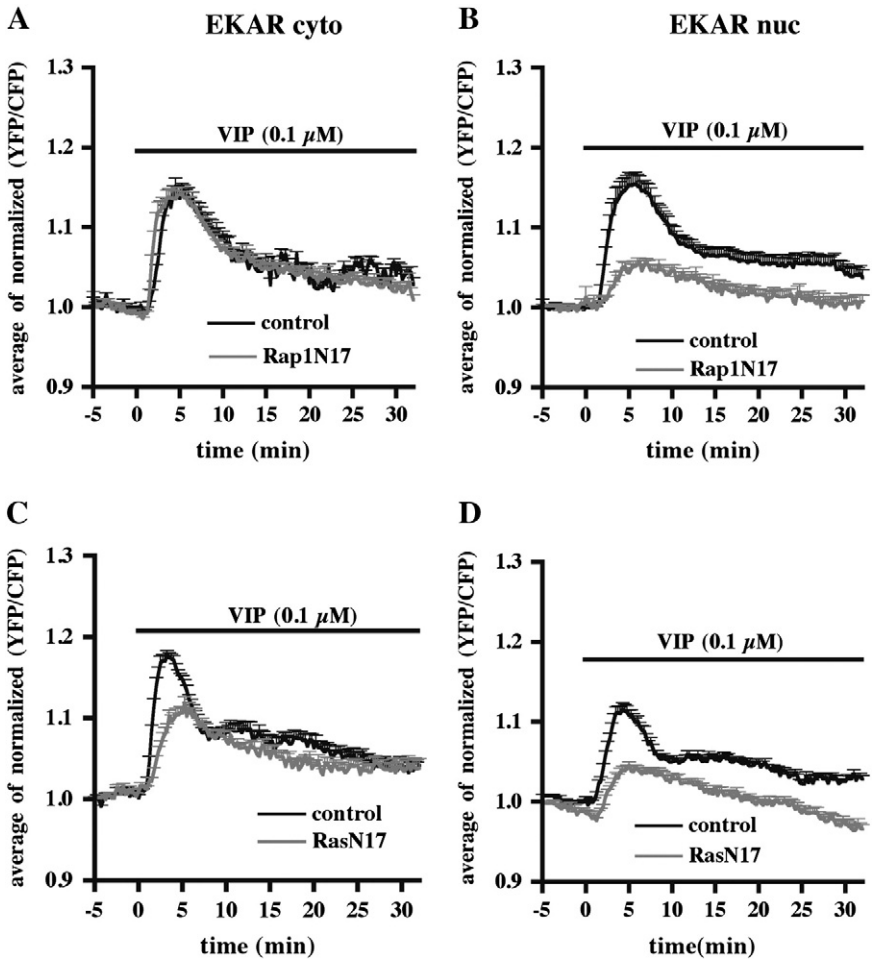

Fig. 10. Ras and Rap1 control VIP-dependent spatiotemporal ERK activation. GH4C1 cells were cotransfected with $EKAR_{cyto}$ (A, C) and pRK5Rap1N17 (A) or pCDNA3.1RasN17 (C) or the respective empty vectors (control in A, C) or with $EKAR_{nuc}$ (B, D) and pRK5Rap1N17 (B) or pCDNA3.1RasN17 (D) or the respective empty vectors (control in B, D). Cells were treated with 0.1 μM VIP as indicated. Single cell recordings were performed on at least 30 cells for each condition. Traces represent the mean ± SEM of single cell recordings.

dynamic of activated ERK and its tight control by the GTPases Ras and Rap1, described in this report, would promote activation of transcriptional regulators in a combinatorial fashion that play a crucial role in the physiological regulation of pituitary hormonal transcription. We have recently established that expression of the gsp oncogene (observed in somatotroph adenomas) initiates a PKA-dependent sustained ERK activation and hormonal hypersecretion. In this pathological context, Ras is switched from being a repressor of cAMP/ERK-sensitive PRL gene control exerted by neuropeptides to an activator of the PRL promoter [49]. Thus, alterations of Ras-dependent spatiotemporal ERK dynamic might promote the development of diseases. Therefore, elucidation of the spatiotemporal complexity of ERK signalling networks should unravel novel therapeutic targets.

Disclosure statement

The authors have nothing to declare and all authors have approved the final article.

Acknowledgements

This work was supported by: Centre National pour la Recherche Scientifique (UMR 7286), Aix-Marseille Université, Association pour le Développement des Recherches Biologiques et Médicales au Centre Hospitalier Régional de Marseille (ADEREM), Novo Nordisk laboratory and Société Française d'Endocrinologie (SFE). C. Zeiller was a recipient of a post-doctoral fellowship from Centre National pour la Recherche Scientifique 2008–2009 and from Pfizer. M. Pertuit was a recipient of a fellowship from La Ligue Contre le Cancer 2009.

We would like to express our gratitude to Dr J.L Bos (University Medical Center Utrecht, The Netherlands) for the gift of pRSVH17 plasmid. pRK5Rap1N17 was a generous gift of T. Bouschet (Centre de Pharmacologie-Endocrinologie, Montpellier, France) and pcDNA.I/HA-ERK1 was a generous gift of G. Pagès, (Centre Antoine Lacassagne, Nice, France). pEYFP-ERK was kindly provided by A.S Show (Washington University School of Medicine, St Louis, MO, USA) and pCMV HA-MEK was a generous gift of D. Romano (University College Dublin, Ireland). We thank Karine Magalon (IBDML, Marseille, France) for the preparation of the pCDNA3.1RasN17 construct.

References

[1] C. Widmann, S. Gibson, M.B. Jarpe, G.L. Johnson, Physiological Reviews 79 (1999) 143–180.
[2] T.P. Garrington, G.L. Johnson, Current Opinion in Cell Biology 11 (1999) 211–218.
[3] S. Yoon, R. Seger, Growth Factors 24 (2006) 21–44.
[4] Z.G. Goldsmith, D.N. Dhanasekaran, Oncogene 26 (2007) 3122–3142.
[5] S. Meloche, J. Pouyssegur, Oncogene 26 (2007) 3227–3239.
[6] M.C. Lawrence, A. Jivan, C. Shao, L. Duan, D. Goad, E. Zaganjor, J. Osborne, K. McGlynn, S. Stippec, S. Earnest, W. Chen, M.H. Cobb, Cell Research 18 (2008) 436–442.

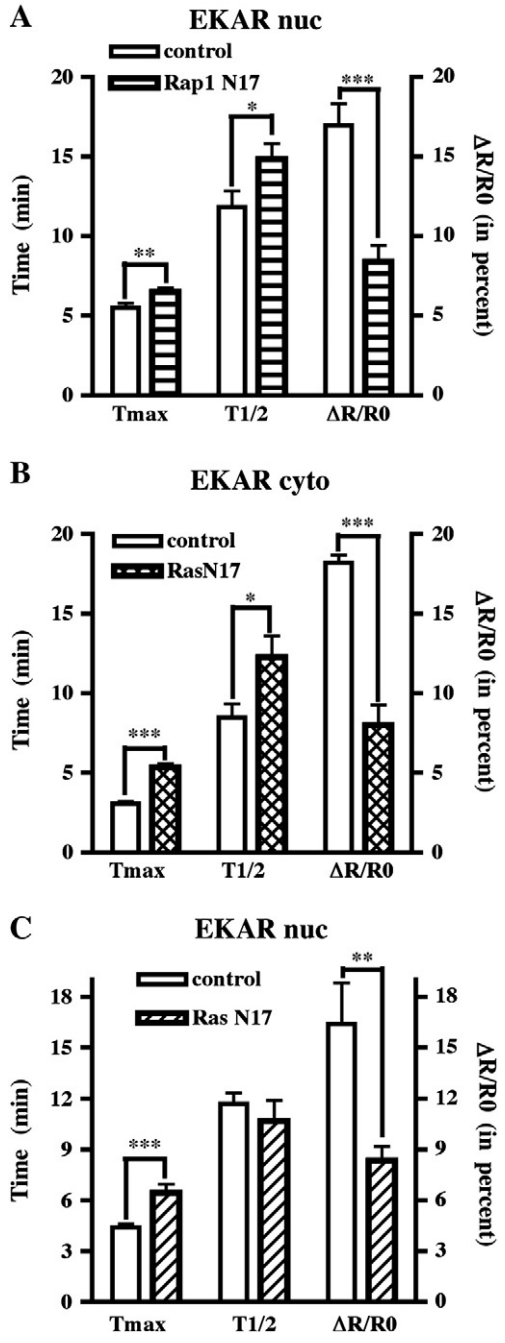

Fig. 11. Quantification of the kinetic parameters of $EKAR_{cyto}$ and $EKAR_{nuc}$ responses to VIP in GH4C1 Rap1N17 or RasN17 expressing cells. Single cell recordings of GH4C1 cells coexpressing (A) $EKAR_{nuc}$ and pRK5Rap1N17 or the empty vector pRK5 (control); (B) $EKAR_{cyto}$ and pCDNA3.1RasN17 or the empty vector pCDNA3.1 (control); (C) $EKAR_{nuc}$ and pCDNA3.1RasN17 or the empty vector pCDNA3.1 (control) were performed and cells were treated with 0.1 μM VIP as described in Fig. 10 on at least 30 cells for each condition. The kinetic parameters Tmax, T1/2 and ΔR/R0 were calculated as described in the Materials and methods and were given as mean ± SEM. (*) $p<0.05$; (**) $p<0.01$; (***) $p<0.001$.

[7] A.S. Dhillon, S. Hagan, O. Rath, W. Kolch, Oncogene 26 (2007) 3279–3290.
[8] J. Pouyssegur, P. Lenormand, European Journal of Biochemistry 270 (2003) 3291–3299.
[9] M. Ebisuya, K. Kondoh, E. Nishida, Journal of Cell Science 118 (2005) 2997–3002.
[10] L.O. Murphy, J. Blenis, Trends in Biochemical Sciences 31 (2006) 268–275.
[11] B.N. Kholodenko, J.F. Hancock, W. Kolch, Nature Reviews. Molecular Cell Biology 11 (2010) 414–426.
[12] A. von Kriegsheim, D. Baiocchi, M. Birtwistle, D. Sumpton, W. Bienvenut, N. Morrice, K. Yamada, A. Lamond, G. Kalna, R. Orton, D. Gilbert, W. Kolch, Nature Cell Biology 11 (2009) 1458–1464.
[13] E. Formstecher, J.W. Ramos, M. Fauquet, D.A. Calderwood, J.C. Hsieh, B. Canton, X.T. Nguyen, J.V. Barnier, J. Camonis, M.H. Ginsberg, H. Chneiweiss, Developmental Cell 1 (2001) 239–250.
[14] S. Torii, M. Kusakabe, T. Yamamoto, M. Maekawa, E. Nishida, Developmental Cell 7 (2004) 33–44.
[15] D.N. Dhanasekaran, K. Kashef, C.M. Lee, H. Xu, E.P. Reddy, Oncogene 26 (2007) 3185–3202.
[16] W.R. Burack, A.S. Shaw, Journal of Biological Chemistry 280 (2005) 3832–3837.
[17] M. Costa, M. Marchi, F. Cardarelli, A. Roy, F. Beltram, L. Maffei, G.M. Ratto, Journal of Cell Science 119 (2006) 4952–4963.
[18] E. Zehorai, Z. Yao, A. Plotnikov, R. Seger, Molecular and Cellular Endocrinology 314 (2010) 213–220.
[19] A. Plotnikov, D. Chuderland, Y. Karamansha, O. Livnah, R. Seger, Molecular and Cellular Biology 31 (2011) 3515–3530.
[20] W. Kolch, Nature Reviews. Molecular Cell Biology 6 (2005) 827–837.
[21] C.J. Caunt, S.P. Armstrong, C.A. Rivers, M.R. Norman, C.A. McArdle, Journal of Biological Chemistry 283 (2008) 26612–26623.
[22] P.J. Stork, J.M. Schmitt, Trends in Cell Biology 12 (2002) 258–266.
[23] S. Kao, R.K. Jaiswal, W. Kolch, G.E. Landreth, Journal of Biological Chemistry 276 (2001) 18169–18177.
[24] S. Sasagawa, Y. Ozaki, K. Fujita, S. Kuroda, Nature Cell Biology 7 (2005) 365–373.
[25] C.M. Cheng, H. Li, S. Gasman, J. Huang, R. Schiff, E.C. Chang, Molecular and Cellular Biology 31 (2011) 983–997.
[26] Y.H. Wang, R.A. Maurer, Molecular Endocrinology 13 (1999) 1094–1104.
[27] H. Kanasaki, T. Yonehara, H. Yamamoto, Y. Takeuchi, K. Fukunaga, K. Takahashi, K. Miyazaki, E. Miyamoto, Biology of Reproduction 67 (2002) 107–113.
[28] D. Romano, M. Pertuit, R. Rasolonjanahary, J.V. Barnier, K. Magalon, A. Enjalbert, C. Gerard, Endocrinology 147 (2006) 6036–6045.
[29] C. Le Pechon-Vallee, K. Magalon, R. Rasolonjanahary, A. Enjalbert, C. Gerard, Neuroendocrinology 72 (2000) 46–56.
[30] P. Kievit, J.D. Lauten, R.A. Maurer, Molecular Endocrinology 15 (2001) 614–624.
[31] T. Yonehara, H. Kanasaki, H. Yamamoto, K. Fukunaga, K. Miyazaki, E. Miyamoto, Endocrinology 142 (2001) 2811–2819.
[32] D. Romano, K. Magalon, A. Ciampini, C. Talet, A. Enjalbert, C. Gerard, Journal of Biological Chemistry 278 (2003) 51386–51394.
[33] C.D. Harvey, A.G. Ehrhardt, C. Cellurale, H. Zhong, R. Yasuda, R.J. Davis, K. Svoboda, Proceedings of the National Academy of Sciences of the United States of America 105 (2008) 19264–19269.
[34] R.H. Medema, R. Wubbolts, J.L. Bos, Molecular and Cellular Biology 11 (1991) 5963–5967.
[35] S. Meloche, G. Pages, J. Pouyssegur, Molecular Biology of the Cell 3 (1992) 63–71.
[36] T. Bouschet, V. Perez, C. Fernandez, J. Bockaert, A. Eychene, L. Journot, Journal of Biological Chemistry 278 (2003) 4778–4785.
[37] A.M. Horgan, P.J. Stork, Experimental Cell Research 285 (2003) 208–220.
[38] C.A. Pickett, A. Gutierrez-Hartmann, Proceedings of the National Academy of Sciences of the United States of America 91 (1994) 8612–8616.
[39] J. Fombonne, S. Reix, R. Rasolonjanahary, E. Danty, S. Thirion, G. Laforge-Anglade, O. Bosler, P. Mehlen, A. Enjalbert, S. Krantic, Molecular Biology of the Cell 15 (2004) 4938–4948.
[40] S.R. Rawlings, I. Piuz, W. Schlegel, J. Bockaert, L. Journot, Endocrinology 136 (1995) 2088–2098.
[41] R.M. Wolthuis, N.D. de Ruiter, R.H. Cool, J.L. Bos, EMBO Journal 16 (1997) 6748–6761.
[42] G.S. Baillie, FEBS Journal 276 (2009) 1790–1799.
[43] A.J. Laude, A.W. Simpson, FEBS Journal 276 (2009) 1800–1816.
[44] J. Omerovic, I.A. Prior, FEBS Journal 276 (2009) 1817–1825.
[45] A. Fujioka, K. Terai, R.E. Itoh, K. Aoki, T. Nakamura, S. Kuroda, E. Nishida, M. Matsuda, Journal of Biological Chemistry 281 (2006) 8917–8926.
[46] M. Sato, Y. Kawai, Y. Umezawa, Analytical Chemistry 79 (2007) 2570–2575.
[47] K.J. Herbst, M.D. Allen, J. Zhang, Molecular and Cellular Biology 31 (2011) 4063–4075.
[48] G.T. Ooi, N. Tawadros, R.M. Escalona, Molecular and Cellular Endocrinology 228 (2004) 1–21.
[49] M. Pertuit, D. Romano, C. Zeiller, A. Barlier, A. Enjalbert, C. Gerard, Endocrinology 152 (2011) 1234–1243.
[50] C. Blanco-Aparicio, J. Torres, R. Pulido, The Journal of Cell Biology 147 (1999) 1129–1136.
[51] N. Mochizuki, S. Yamashita, K. Kurokawa, Y. Ohba, T. Nagai, A. Miyawaki, M. Matsuda, Nature 411 (2001) 1065–1068.
[52] Y. Ohba, K. Kurokawa, M. Matsuda, EMBO Journal 22 (2003) 859–869.
[53] A. Mor, M.R. Philips, Annual Review of Immunology 24 (2006) 771–800.
[54] N. Fehrenbacher, D. Bar-Sagi, M. Philips, Molecular Oncology 3 (2009) 297–307.
[55] M. Russell, C.A. Lange-Carter, G.L. Johnson, Journal of Biological Chemistry 270 (1995) 11757–11760.
[56] W. Li, M. Han, K.L. Guan, Genes & Development 14 (2000) 895–900.
[57] B. Casar, I. Arozarena, V. Sanz-Moreno, A. Pinto, L. Agudo-Ibanez, R. Marais, R.E. Lewis, M.T. Berciano, P. Crespo, Molecular and Cellular Biology 29 (2009) 1338–1353.
[58] Y. Zhang, D.B. Moheban, B.R. Conway, A. Bhattacharyya, R.A. Segal, Journal of Neuroscience 20 (2000) 5671–5678.
[59] S. Xiong, Q. Zhao, Z. Rong, G. Huang, Y. Huang, P. Chen, S. Zhang, L. Liu, Z. Chang, Journal of Biological Chemistry 278 (2003) 50273–50282.

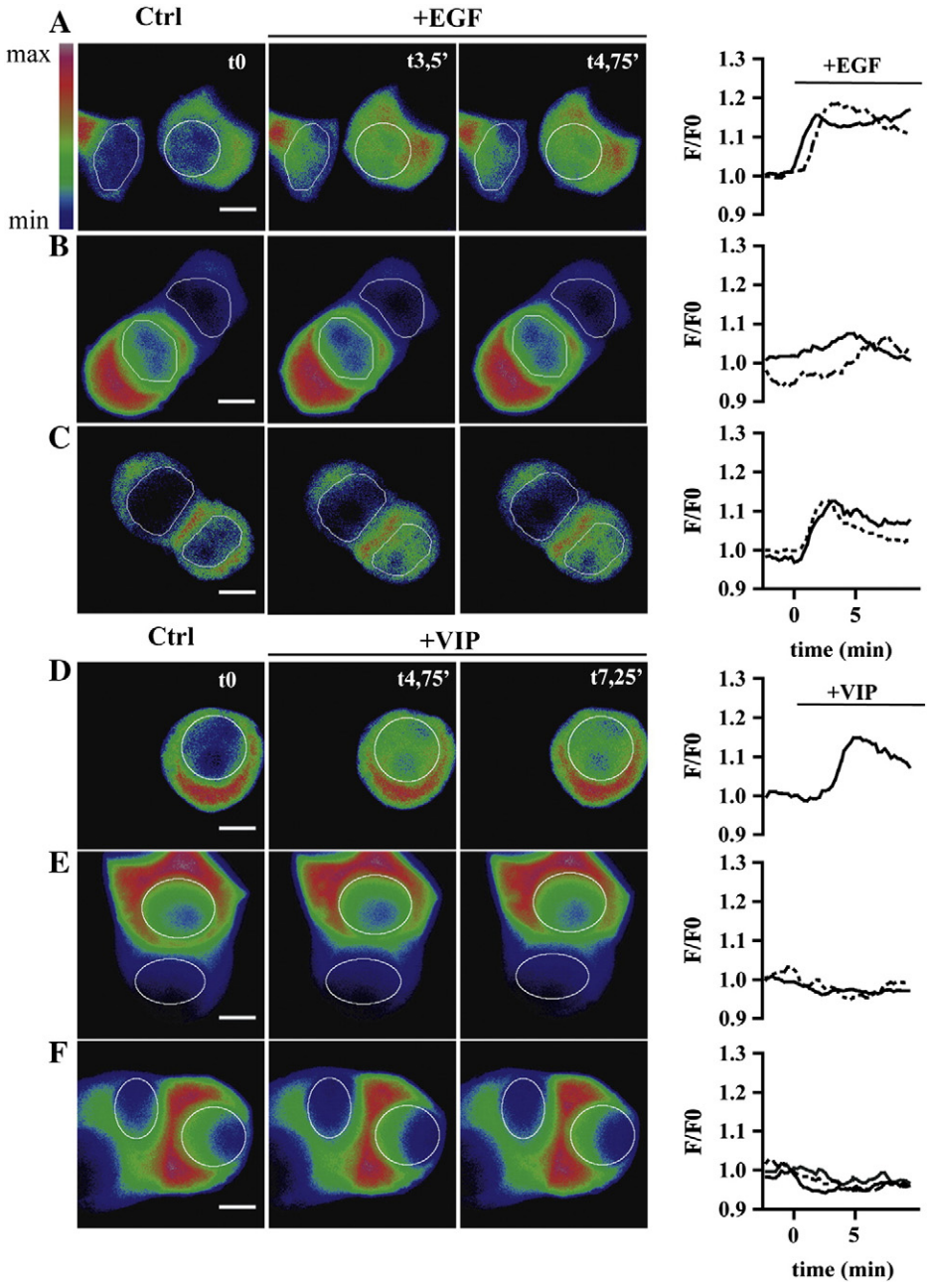

Fig. 12. Differential control of ERK nuclear translocation by Ras and Rap1. GH4C1 cells coexpressing pEYFP-ERK, pCMV-HA-MEK and (A) pCDNA3.1 or (B, E) pCDNA3.1RasN17 or (D) pRK5 or (C, F) pRK5Rap1N17 were treated as indicated (A, B, C) with 1 nM EGF or (D, E, F) with 0.1 μM VIP. (Left panels) Pseudocolour images of the YFP-ERK emission intensity were given. A white line outlines the nucleus of each cell. (Right panels) Traces represent the time course of YFP-ERK fluorescence in the nucleus of cells presented in the left panels as described in the Materials and methods. As similar translocation was observed in cells transfected with the different empty vectors under each treatment, results for one empty vector were presented for each treatment. YFP-ERK fluorescence of representative cells was given. Scale bar: 5 μm.

[60] J. Muller, A.M. Cacace, W.E. Lyons, C.B. McGill, D.K. Morrison, Molecular and Cellular Biology 20 (2000) 5529–5539.
[61] N. Billestrup, L.W. Swanson, W. Vale, Proceedings of the National Academy of Sciences of the United States of America 83 (1986) 6854–6857.
[62] D. Gourdji, D. Bataille, N. Vauclin, D. Grouselle, G. Rosselin, A. Tixier-Vidal, FEBS Letters 104 (1979) 165–168.